Available online at www.sciencedirect.com
SCIENCE DIRECT®
Computers and Structures 83 (2005) 267–278
Computers & Structures
www.elsevier.com/locate/compstruc

The method of fundamental solutions for the Cauchy problem associated with two-dimensional Helmholtz-type equations

Liviu Marin [a,*], Daniel Lesnic [b]

[a] School of the Environment, University of Leeds, Woodhouse Lane, Leeds LS2 9JT, UK
[b] Department of Applied Mathematics, University of Leeds, Leeds LS2 9JT, UK

Received 16 September 2004; accepted 21 October 2004
Available online 19 December 2004

Abstract

In this paper, the application of the method of fundamental solutions to the Cauchy problem associated with two-dimensional Helmholtz-type equations is investigated. The resulting system of linear algebraic equations is ill-conditioned and therefore its solution is regularized by employing the first-order Tikhonov functional, while the choice of the regularization parameter is based on the L-curve method. Numerical results are presented for both smooth and piecewise smooth geometries. The convergence and the stability of the method with respect to increasing the number of source points and the distance between the source points and the boundary of the solution domain, and decreasing the amount of noise added into the input data, respectively, are analysed.

Keywords: Meshless method; Method of fundamental solutions; Cauchy problem; Helmholtz-type equations; Regularization; Inverse problem

1. Introduction

The method of fundamental solutions (MFS) was originally introduced by Kupradze and Aleksidze [1], whilst its numerical formulation was first given by Mathon and Johnston [2]. The main idea of the MFS consists in approximating the solution of the problem by a linear combination of fundamental solutions with respect to some singularities/source points which are located outside the domain. Then the original problem is reduced to determining the unknown coefficients of the fundamental solutions and the coordinates of the source points by requiring the approximation to satisfy the boundary conditions and hence solving a nonlinear problem. If the source points are a priori fixed then the coefficients of the MFS approximation are determined by solving a linear problem. An excellent survey of the MFS and related methods over the past three decades has been presented by Fairweather and Karageorghis [3].

The advantages of the MFS over domain discretisation methods, such as the finite-difference (FDM) and the finite element methods (FEM), are very well-documented, see e.g. Fairweather and Karageorghis [3]. In addition, the MFS has all the advantages of boundary methods, such as the boundary element method

* Corresponding author. Tel.: +44 113 3436744; fax: +44 113 3436716.
E-mail address: liviu@env.leeds.ac.uk (L. Marin).

0045-7949/$ - see front matter © 2004 Elsevier Ltd. All rights reserved.
doi:10.1016/j.compstruc.2004.10.005

(BEM), as well as several advantages over other boundary methods. For example, the MFS does not require an elaborate discretisation of the boundary, integrations over the boundary are avoided, the solution in the interior of the domain is evaluated without extra quadratures, its implementation is very easy and only little data preparation is required. The most arguable issue regarding the MFS is still the location of the source points. However, this problem can be overcome by employing a nonlinear least-squares minimisation procedure. Alternatively, the source points can be prescribed a priori, see [4–6], and the post-processing analysis of the errors can indicate their optimal location.

The MFS has been successfully applied to solving a wide variety of boundary value problems. Karageorghis and Fairweather [7] have solved numerically the biharmonic equation using the MFS and later their method has been modified in order to take into account the presence of boundary singularities in both the Laplace and the biharmonic equations by Poullikkas et al. [8]. Furthermore, Poullikkas et al. [9] have investigated the numerical solutions of the inhomogeneous harmonic and biharmonic equations by reducing these problems to the homogeneous corresponding cases and subtracting a particular solution of the governing equation. The MFS has been formulated for three-dimensional Signorini boundary value problems and it has been tested on a three-dimensional electropainting problem related to the coating of vehicle roofs in Poullikkas et al. [10]. Whilst Karageorghis and Fairweather [11] have studied the use of the MFS for the approximate solution of three-dimensional isotropic materials with axisymmetrical geometry and both axisymmetrical and arbitrary boundary conditions. The application of the MFS to two-dimensional problems of steady-state heat conduction and elastostatics in isotropic and anisotropic bimaterials has been addressed by Berger and Karageorghis [12,13]. Karageorghis [14] has investigated the calculation of the eigenvalues of the Helmholtz equation subject to homogeneous Dirichlet boundary conditions for circular and rectangular geometries by employing the MFS, whilst Poullikkas et al. [15] have successfully applied the MFS for solving three-dimensional elastostatics problems. The MFS, in conjunction with singular value decomposition, has been employed by Ramachandran [16] in order to obtain numerical solutions of the Laplace and the Helmholtz equations. Recently, Balakrishnan et al. [17] have proposed an operator splitting-radial basis function method as a generic solution procedure for transient nonlinear Poisson problems by combining the concepts of operator splitting, radial basis function interpolation, particular solutions and the MFS.

Helmholtz-type equations arise naturally in many physical applications related to wave propagation and vibration phenomena. They are often used to describe the vibration of a structure [18], the acoustic cavity problem [19], the radiation wave [20], the scattering of a wave [21] and the heat conduction in fins [22]. The knowledge of the Dirichlet, Neumann or mixed boundary conditions on the entire boundary of the solution domain gives rise to direct problems for Helmholtz-type equations which have been extensively studied in the literature, see for example [23–25]. Unfortunately, many engineering problems do not belong to this category. In particular, the boundary conditions are often incomplete, either in the form of underspecified and overspecified boundary conditions on different parts of the boundary or the solution is prescribed at some internal points in the domain. These are inverse problems, and it is well-known that they are generally ill-posed, i.e. the existence, uniqueness and stability of their solutions are not always guaranteed, see e.g. Hadamard [26].

A classical example of an inverse problem for Helmholtz-type equations is the Cauchy problem in which boundary conditions for both the solution and its normal derivative are prescribed only on a part of the boundary of the solution domain, whilst no information is available on the remaining part of the boundary. Unlike in direct problems, the uniqueness of the Cauchy problem is guaranteed without the necessity of removing the eigenvalues for the Laplacian. A BEM-based acoustic holography technique using the singular value decomposition (SVD) for the reconstruction of sound fields generated by irregularly shaped sources has been developed by Bai [27]. The vibrational velocity, sound pressure and acoustic power on the vibrating boundary comprising an enclosed space have been reconstructed by Kim and Ih [28] who have used the SVD in order to obtain the inverse solution in the least-squares sense and to express the acoustic modal expansion between the measurement and source field. Wang and Wu [29] have developed a method employing the spherical wave expansion theory and a least-squares minimisation to reconstruct the acoustic pressure field from a vibrating object and their method has been extended to the reconstruction of acoustic pressure fields inside the cavity of a vibrating object by Wu and Yu [30]. DeLillo et al. [31] have detected the source of acoustical noise inside the cabin of a midsize aircraft from measurements of the acoustical pressure field inside the cabin by solving a linear Fredholm integral equation of the first kind. Recently, Marin et al. [32,33] have solved the Cauchy problem for Helmholtz-type equations by employing the BEM in conjunction with an alternating iterative algorithm and the conjugate gradient method, respectively.

To our knowledge, the application of the MFS to the Cauchy problem associated with Helmholtz-type equations has not been investigated yet. The MFS discretised system of equations is ill-conditioned and hence it is solved by employing the first-order Tikhonov regularization method, see e.g. Tikhonov and Arsenin [34], whilst the choice of the regularization parameter is based

on the L-curve criterion, see Hansen [35]. Three examples for the two-dimensional Helmholtz and modified Helmholtz equations in both smooth and piecewise smooth domains are investigated. In addition, the convergence and stability of the method with respect to the location and the number of source points and the amount of noise added into the Cauchy input data, respectively, are analysed.

2. Mathematical formulation

Consider an open bounded domain $\Omega \subset \mathbb{R}^2$ and assume that Ω is bounded by a piecewise smooth boundary $\Gamma \equiv \partial\Omega$, such that $\Gamma = \overline{\Gamma}_1 \cup \overline{\Gamma}_2$, where $\Gamma_1, \Gamma_2 \neq \emptyset$ and $\Gamma_1 \cap \Gamma_2 = \emptyset$. Referring to heat transfer for the sake of the physical explanation, we assume that the temperature field $T(\boldsymbol{x})$ satisfies the Helmholtz-type equation in the domain Ω, namely

$$(\Delta + k^2)T(\boldsymbol{x}) = 0, \quad \boldsymbol{x} \in \Omega, \tag{1}$$

where $k = \alpha + \mathrm{i}\beta \in \mathbb{C}$, $\mathrm{i} = \sqrt{-1}$. For example, when $\alpha = 0$ and $\beta \in \mathbb{R}$, the partial differential Eq. (1) models the heat conduction in a fin [22] where T is the dimensionless local fin temperature, $\beta^2 = h/(\widetilde{k}t)$, h is the surface heat transfer coefficient (W/(m^2 K)), $\widetilde{k}$ is the thermal conductivity of the fin (W/(m K)) and t is the half-fin thickness (m).

Let $\boldsymbol{n}(\boldsymbol{x})$ be the outward unit normal vector at Γ and $\Phi(\boldsymbol{x}) \equiv (\nabla T \cdot \boldsymbol{n})(\boldsymbol{x})$ be the flux at a point $\boldsymbol{x} \in \Gamma$. In the direct problem formulation, the knowledge of the temperature and/or flux on the whole boundary Γ gives the corresponding Dirichlet, Neumann, or mixed boundary conditions which enables us to determine the temperature distribution in the domain Ω. If it is possible to measure both the temperature and the flux on a part of the boundary Γ, say Γ_1, then this leads to the mathematical formulation of an inverse problem consisting of Eq. (1) and the boundary conditions

$$T(\boldsymbol{x}) = \widetilde{T}(\boldsymbol{x}), \quad \Phi(\boldsymbol{x}) = \widetilde{\Phi}(\boldsymbol{x}), \quad \boldsymbol{x} \in \Gamma_1, \tag{2}$$

where $\widetilde{T}$ and $\widetilde{\Phi}$ are prescribed functions and $\Gamma_1 \subset \Gamma$, meas$(\Gamma_1) > 0$. In the above formulation of the boundary conditions (2), it can be seen that the boundary Γ_1 is overspecified by prescribing both the temperature $T|_{\Gamma_1}$ and the flux $\Phi|_{\Gamma_1}$, whilst the boundary Γ_2 is underspecified since both the temperature $T|_{\Gamma_2}$ and the flux $\Phi|_{\Gamma_2}$ are unknown and have to be determined. It should be noted that the problem studied in this paper is of practical importance. For example, the Cauchy problem (1) and (2), where $k \in \mathbb{C} \setminus \mathbb{R}$, represents the mathematical model for the heat conduction in plate finned-tube heat exchangers [22] for which the temperature and the flux can be measured at some points on the fin, whilst both the temperature and the flux are unknown at the fin base or, equivalently, in the tubes.

This problem, termed the Cauchy problem, is much more difficult to solve both analytically and numerically than the direct problem, since the solution does not satisfy the general conditions of well-posedness. Whilst the Dirichlet, Neumann or mixed direct problems associated to Eq. (1) do not always have a unique solution due to the eigensolutions, see Chen and Zhou [36], the solution of the Cauchy problem given by Eqs. (1) and (2) is unique based on the analytical continuation property. However, it is well-known that if this solution exists then it is unstable with respect to small perturbations in the data on Γ_2, see e.g. Hadamard [26]. Thus the problem under investigation is ill-posed and we cannot use a direct approach, such as the Gauss elimination method, in order to solve the system of linear equations which arises from the discretisation of the partial differential equations (1) and the boundary conditions (2). Therefore, regularization methods are required in order to solve accurately the Cauchy problem associated with Helmholtz-type equations.

3. Method of fundamental solutions and regularization

The fundamental solutions $\mathscr{F}_{\mathrm{H}}$ and $\mathscr{F}_{\mathrm{MH}}$ of the Helmholtz ($k \in \mathbb{R}$) and the modified Helmholtz ($k \in \mathbb{C} \setminus \mathbb{R}$) Eq. (1), respectively, in the two-dimensional case are given by, see e.g. Fairweather and Karageorghis [3],

$$\mathscr{F}_{\mathrm{H}}(\boldsymbol{x}, \boldsymbol{y}) = \frac{\mathrm{i}}{4} H_0^{(1)}(kr(\boldsymbol{x}, \boldsymbol{y})), \quad \boldsymbol{x} \in \overline{\Omega}, \ \boldsymbol{y} \in \mathbb{R}^2 \setminus \overline{\Omega}, \tag{3}$$

$$\mathscr{F}_{\mathrm{MH}}(\boldsymbol{x}, \boldsymbol{y}) = \frac{1}{2\pi} K_0(kr(\boldsymbol{x}, \boldsymbol{y})), \quad \boldsymbol{x} \in \overline{\Omega}, \ \boldsymbol{y} \in \mathbb{R}^2 \setminus \overline{\Omega}, \tag{4}$$

where $r(\boldsymbol{x}, \boldsymbol{y}) = \sqrt{(x_1 - y_1)^2 + (x_2 - y_2)^2}$ represents the distance between the domain point $\boldsymbol{x} = (x_1, x_2)$ and the source point $\boldsymbol{y} = (y_1, y_2)$, $H_0^{(1)}$ is the Hankel function of the first kind of order zero and K_0 is the modified Bessel function of the second kind of order zero.

The main idea of the MFS consists of the approximation of the temperature in the solution domain by a linear combination of fundamental solutions with respect to M source points $\boldsymbol{y}_j$ in the form

$$T(\boldsymbol{x}) \approx T^M(\boldsymbol{a}, \boldsymbol{Y}; \boldsymbol{x}) = \sum_{j=1}^{M} a_j \mathscr{F}(\boldsymbol{x}, \boldsymbol{y}^j), \quad \boldsymbol{x} \in \overline{\Omega}, \tag{5}$$

where $\mathscr{F} = \mathscr{F}_{\mathrm{H}}$ in the case of the Helmholtz equation, $\mathscr{F} = \mathscr{F}_{\mathrm{MH}}$ in the case of the modified Helmholtz equation, $\boldsymbol{a} = (a_1, \ldots, a_M)$ and $\boldsymbol{Y}$ is a $2M$-vector containing the coordinates of the source points $\boldsymbol{y}^j$, $j = 1, \ldots, M$. Then the flux can be approximated on the boundary Γ by

$$\Phi(\boldsymbol{x}) \approx \Phi^M(\boldsymbol{a}, \boldsymbol{Y}, \boldsymbol{n}; \boldsymbol{x}) = \sum_{j=1}^{M} a_j \mathscr{G}(\boldsymbol{x}, \boldsymbol{y}^j; \boldsymbol{n}), \quad \boldsymbol{x} \in \Gamma, \tag{6}$$

where $\mathscr{G}(\boldsymbol{x},\boldsymbol{y};\boldsymbol{n}) = \nabla_x \mathscr{F}(\boldsymbol{x},\boldsymbol{y})\cdot\boldsymbol{n}(\boldsymbol{x})$ and $\mathscr{G}_{\mathrm{H}}$ in the case of the Helmholtz equation and $\mathscr{G}_{\mathrm{MH}}$ in the case of the modified Helmholtz equation are given by

$$\mathscr{G}_{\mathrm{H}}(\boldsymbol{x},\boldsymbol{y};\boldsymbol{n}) = -\frac{((\boldsymbol{x}-\boldsymbol{y})\cdot\boldsymbol{n}(\boldsymbol{x}))ki}{4r(\boldsymbol{x},\boldsymbol{y})}H_1^{(1)}(kr(\boldsymbol{x},\boldsymbol{y})),\quad \boldsymbol{x}\in\Gamma,\ \ \boldsymbol{y}\in\mathbb{R}^2\setminus\overline{\Omega}, \tag{7}$$

$$\mathscr{G}_{\mathrm{MH}}(\boldsymbol{x},\boldsymbol{y};\boldsymbol{n}) = -\frac{((\boldsymbol{x}-\boldsymbol{y})\cdot\boldsymbol{n}(\boldsymbol{x}))k}{2\pi r(\boldsymbol{x},\boldsymbol{y})}K_1(kr(\boldsymbol{x},\boldsymbol{y})),\quad \boldsymbol{x}\in\Gamma,\ \ \boldsymbol{y}\in\mathbb{R}^2\setminus\overline{\Omega}. \tag{8}$$

Here $H_1^{(1)}$ is the Hankel function of the first kind of order one and K_1 is the modified Bessel function of the second kind of order one.

If the solution domain is a disk of radius r, it was shown in [37,38] that, when the collocation and source points are placed uniformly on the boundary of the disk and on a circle of radius R, $R > r$, respectively, then the error in the MFS approximation for N collocation points and N singularities satisfies $\sup_{x\in\Omega}|T(\boldsymbol{x}) - T^N(\boldsymbol{x})| = \mathrm{O}((r/R)^N)$, i.e. exponential convergence is achieved. Furthermore, this result was generalised to two-dimensional regions whose boundaries are analytic Jordan curves by Katsurada [39,40]. It is worth mentioning that the functional approximation given by Eq. (5) is also consistent, in the sense that this functional also approximates accurately the exact solution of the problem not only on the boundary Γ, but also in the interior of the solution domain Ω, see Kondepalli et al. [41] and MacDonell [42]. Moreover, the MFS approximation (5) is capable of reproducing various types of solutions to Helmholtz-type equations, such as constant, linear, quadratic, exponential, trigonometric functions, etc., see e.g. Fairweather and Karageorghis [3] and Golberg and Chen [6].

If N collocation points $\boldsymbol{x}^l$, $l = 1,\ldots,N$, are chosen on the overspecified boundary Γ_1 and the location of the source points $\boldsymbol{y}^j$, $j = 1,\ldots,M$, is set then Eqs. (5) and (6) recast as a system of $2N$ linear algebraic equations with M unknowns which can be generically written as

$$\mathbb{A}\boldsymbol{X} = \boldsymbol{F}, \tag{9}$$

where the MFS matrix $\mathbb{A}$, the unknown vector $\boldsymbol{X}$ and the right-hand side vector $\boldsymbol{F}$ are given by

$$\begin{aligned} &A_{l,j} = \mathscr{F}(\boldsymbol{x}^l,\boldsymbol{y}^j),\quad A_{N+l,j} = \mathscr{G}(\boldsymbol{x}^l,\boldsymbol{y}^j),\quad X_j = a_j,\\ &F_l = T(\boldsymbol{x}^l),\quad F_{N+l} = \Phi(\boldsymbol{x}^l),\\ &\quad l = 1,\ldots,N,\quad j = 1,\ldots,M. \end{aligned} \tag{10}$$

It should be noted that in order to uniquely determine the solution $\boldsymbol{X}$ of the system of linear algebraic Eq. (9), i.e. the coefficients a_j, $j = 1,\ldots,M$, in the approximations (5) and (6), the number N of boundary collocation points and the number M of source points must satisfy the inequality $M \leqslant 2N$. However, the system of linear algebraic Eq. (9) cannot be solved by direct methods, such as the least-squares method, since such an approach would produce a highly unstable solution due to the large value of the condition number of the matrix $\mathbb{A}$ which increases dramatically as the number of boundary collocation points and source points increases. Several regularization procedures have been developed to solve such ill-conditioned systems, see for example Hansen [43]. However, we only consider the Tikhonov regularization method in our study. For further details on this method see Tikhonov and Arsenin [34].

It should be mentioned that for inverse problems, the resulting systems of linear algebraic equations are ill-conditioned, even if other well-known numerical methods (FDM, FEM or BEM) are employed. Although the MFS system of linear algebraic Eq. (9) is ill-conditioned even when dealing with direct problems, the MFS has no longer this disadvantage in comparison with other numerical methods, in the sense that regularization is required for both direct and inverse problems in order to solve the resulting MFS system. In addition, the MFS preserves its advantages, such as the lack of any mesh, the high accuracy of the numerical results, etc.

The Tikhonov regularized solution to the system of linear algebraic Eq. (9) is sought as

$$\boldsymbol{X}_\lambda : \mathscr{T}_\lambda(\boldsymbol{X}_\lambda) = \min_{\boldsymbol{X}\in\mathbb{R}^M}\mathscr{T}_\lambda(\boldsymbol{X}), \tag{11}$$

where $\mathscr{T}_\lambda$ represents the sth order Tikhonov functional given by

$$\begin{aligned} &\mathscr{T}_\lambda(\cdot) : \mathbb{R}^M \to [0,\infty),\\ &\mathscr{T}_\lambda(\boldsymbol{X}) = \|\mathbb{A}\boldsymbol{X} - \boldsymbol{F}\|_2^2 + \lambda^2\|\mathbb{R}^{(s)}\boldsymbol{X}\|_2^2, \end{aligned} \tag{12}$$

the matrix $\mathbb{R}^{(s)} \in \mathbb{R}^{(M-s)\times M}$ induces a $\mathscr{C}^s$-constraint on the solution $\boldsymbol{X}$ and $\lambda > 0$ is the regularization parameter to be chosen. For example, in the case of the zeroth-, first- and second-order Tikhonov regularization method the matrix $\mathbb{R}^{(s)}$, i.e. $s = 0,1,2$, is given by

$$\mathbb{R}^{(0)} = \begin{bmatrix} 1 & 0 & \ldots & 0\\ 0 & 1 & \ldots & 0\\ \vdots & \vdots & \ddots & \vdots\\ 0 & 0 & \ldots & 1 \end{bmatrix} \in \mathbb{R}^{M\times M},$$

$$\mathbb{R}^{(1)} = \begin{bmatrix} -1 & 1 & 0 & \ldots & 0\\ 0 & -1 & 1 & \ldots & 0\\ \vdots & \vdots & \ddots & \ddots & \vdots\\ 0 & 0 & \ldots & -1 & 1 \end{bmatrix} \in \mathbb{R}^{(M-1)\times M},$$

$$\mathbb{R}^{(2)} = \begin{bmatrix} 1 & -2 & 1 & 0 & \ldots & 0\\ 0 & 1 & -2 & 1 & \ldots & 0\\ \vdots & \vdots & \ddots & \ddots & \ddots & \vdots\\ 0 & 0 & \ldots & 1 & -2 & 1 \end{bmatrix} \in \mathbb{R}^{(M-2)\times M}. \tag{13}$$

Formally, the Tikhonov regularized solution $\boldsymbol{X}_\lambda$ of the problem (11) is given as the solution of the regularized equation

$$(\mathbb{A}^{\mathrm{T}}\mathbb{A} + \lambda^2 \mathbb{R}^{(s)^{\mathrm{T}}}\mathbb{R}^{(s)})\boldsymbol{X} = \mathbb{A}^{\mathrm{T}}\boldsymbol{F}. \tag{14}$$

Regularization is necessary when solving ill-conditioned systems of linear equations because the simple least-squares solution, i.e. $\lambda = 0$, is completely dominated by contributions from data errors and rounding errors. By adding regularization we are able to damp out these contributions and maintain the norm $\|\mathbb{R}^{(s)}\boldsymbol{X}\|_2$ to be of reasonable size. If too much regularization, or damping, i.e. λ^2 is large, is imposed on the solution then it will not fit the given data $\boldsymbol{F}$ properly and the residual norm $\|\mathbb{A}\boldsymbol{X} - \boldsymbol{F}\|_2$ will be too large. If too little regularization is imposed on the solution, i.e. λ^2 is small, then the fit will be good, but the solution will be dominated by the contributions from the data errors, and hence $\|\mathbb{R}^{(s)}\boldsymbol{X}\|_2$ will be too large. It is quite natural to plot the norm of the solution as a function of the norm of the residual parametrised by the regularization parameter λ, i.e. $\{\|\mathbb{A}\boldsymbol{X}_\lambda - \boldsymbol{F}\|_2,\ \|\mathbb{R}^{(s)}\boldsymbol{X}_\lambda\|_2,\ \lambda > 0\}$. Hence, the L-curve is really a trade-off curve between two quantities that both should be controlled and, according to the L-curve criterion, the optimal value λ_{opt} of the regularization parameter λ is chosen at the "corner" of the L-curve, see Hansen [35,43]. To summarize, the Tikhonov regularization method solves a minimisation problem using different smoothness constraints, e.g. see expressions (13) for the matrix $\mathbb{R}^{(s)}$, in order to provide a stable solution which fits the data and also has a minimum structure.

4. Numerical results and discussion

The numerical results presented in this section for the Cauchy problem associated with Helmholtz-type equations indicate that the proposed method is feasible and efficient. In order to assess the performance of the MFS in conjunction with the first-order Tikhonov regularization method, we solve the Cauchy problem (1) and (2) for three typical examples corresponding to Helmholtz-type equations in both smooth and piecewise smooth geometries, see also Fig. 1.

Example 1 (modified Helmholtz equation in a smooth domain). We consider the following analytical solutions for the temperature:

$$T^{(\mathrm{an})}(\boldsymbol{x}) = \exp(\xi_1 x_1 + \xi_2 x_2), \quad \boldsymbol{x} = (x_1, x_2) \in \Omega, \tag{15}$$

in the unit disk $\Omega = \{\boldsymbol{x} = (x_1, x_2) | x_1^2 + x_2^2 < 1\}$, where $k = \alpha + \mathrm{i}\beta$, $\alpha = 0$, $\beta = 2.0$, $\xi_1 = 1.0$ and $\xi_2 = \sqrt{\beta^2 - \xi_1^2}$. Here $\Gamma_1 = \{\boldsymbol{x} \in \Gamma | 0 \leqslant \theta(\boldsymbol{x}) \leqslant \pi/4\}$ and $\Gamma_2 = \{\boldsymbol{x} \in \Gamma | \pi/4 < \theta(\boldsymbol{x}) < 2\pi\}$, where $\theta(\boldsymbol{x})$ is the angular polar coordinate of $\boldsymbol{x}$.

Example 2 (Helmholtz equation in a smooth domain). We consider the following analytical solutions for the temperature:

$$T^{(\mathrm{an})}(\boldsymbol{x}) = \cos(\xi_1 x_1 + \xi_2 x_2), \quad \boldsymbol{x} = (x_1, x_2) \in \Omega, \tag{16}$$

in the unit disk $\Omega = \{\boldsymbol{x} = (x_1, x_2) | x_1^2 + x_2^2 < 1\}$, where $k = \alpha + \mathrm{i}\beta$, $\alpha = 1.0$, $\beta = 0$, $\xi_1 = 0.5$ and $\xi_2 = \sqrt{\alpha^2 - \xi_1^2}$. Here $\Gamma_1 = \{\boldsymbol{x} \in \Gamma | 0 \leqslant \theta(\boldsymbol{x}) \leqslant \pi/2\}$ and $\Gamma_2 = \{\boldsymbol{x} \in \Gamma | \pi/2 < \theta(\boldsymbol{x}) < 2\pi\}$.

Example 3 (Helmholtz equation in a piecewise smooth domain). We consider the following analytical solutions for the temperature:

$$T^{(\mathrm{an})}(\boldsymbol{x}) = \cos(\xi_1 x_1 + \xi_2 x_2), \quad \boldsymbol{x} = (x_1, x_2) \in \Omega, \tag{17}$$

in the square $\Omega = (-1, 1) \times (-1, 1)$, where $k = \alpha + \mathrm{i}\beta$, $\alpha = 2.0$, $\beta = 0$, $\xi_1 = 1.0$ and $\xi_2 = -\sqrt{\alpha^2 - \xi_1^2}$. Here $\Gamma_1 = \{\boldsymbol{x} \in \Gamma | x_1 = \pm 1, -1 \leqslant x_2 \leqslant 1\} \cup \{\boldsymbol{x} \in \Gamma | -1 \leqslant x_1 \leqslant 1, x_2 = 1\}$ and $\Gamma_2 = \{\boldsymbol{x} \in \Gamma | -1 \leqslant x_1 < 1, x_2 = -1\}$.

It should be noted that for the examples considered, the Cauchy data is available on a portion Γ_1 of the boundary Γ such that $\mathrm{meas}(\Gamma_1) = \mathrm{meas}(\Gamma)/4$ in the case of Example 1, $\mathrm{meas}(\Gamma_1) = \mathrm{meas}(\Gamma)/2$ in the case of Example 2 and $\mathrm{meas}(\Gamma_1) = 3\mathrm{meas}(\Gamma)/4$ in the case of Example 3. The Cauchy problems investigated in this study have been solved using a uniform distribution of both the boundary collocation points $\boldsymbol{x}^l$, $l = 1, \ldots, N$, and the source points $\boldsymbol{y}^j$, $j = 1, \ldots, M$, with the mention that the later were located on the boundary of the disk $\mathrm{B}(0, R)$, where the radius $R > 0$ was chosen such that $\overline{\Omega} \subset \mathrm{B}(0, R)$. Furthermore, the number of boundary collocation points was set to $N = 80 \times \mathrm{meas}(\Gamma_1)/\mathrm{meas}(\Gamma)$.

4.1. Stability of the method

In order to investigate the stability of the MFS, the temperature $T|_{\Gamma_1} = T^{(\mathrm{an})}|_{\Gamma_1}$ has been perturbed as $\widetilde{T} = T + \delta T$, where δT is a Gaussian random variable with mean zero and standard deviation $\sigma = \max_{\Gamma_1}|T|(p_T/100)$, generated by the NAG subroutine G05DDF (which generates pseudo-random numbers from a normal/Gaussian distribution with zero mean and specified standard deviation), and $p_T\%$ is the percentage of additive noise included in the input data $T|_{\Gamma_1}$ in order to simulate the inherent measurement errors.

Fig. 2 presents the L-curves obtained for the Cauchy problem given by Example 2 using the first-order Tikhonov regularization method, i.e. $s = 1$ in (12), to solve the MFS system of Eq. (9), $M = 20$ source points, $R = 5.0$ and with various levels of noise. From this figure it can be seen that for each amount of noise considered, the "corner" of the corresponding L-curve can be clearly determined and this gives $\lambda = \lambda_{\mathrm{opt}} = 3.16 \times 10^{-4}$

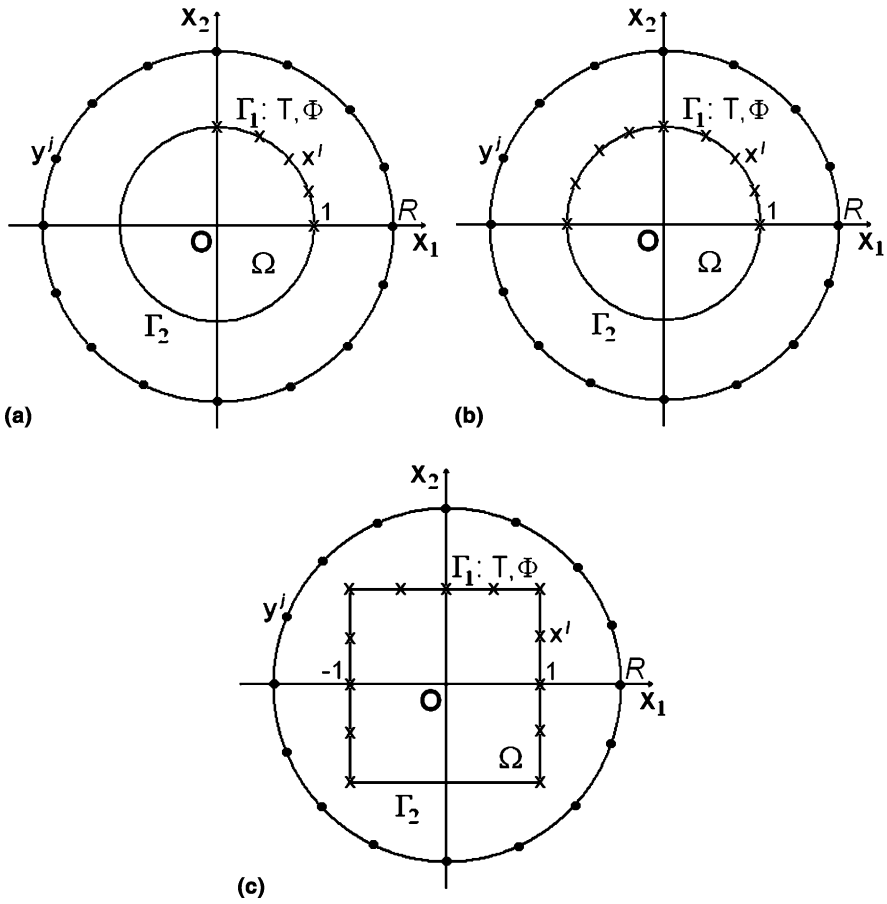

Fig. 1. A schematic diagram of the domain Ω, the boundary conditions and the location of the sources (●) and the collocation points (×), for the Cauchy problem corresponding to (a) Example 1, (b) Example 2, and (c) Example 3.

and $\lambda = \lambda_{\text{opt}} = 1.0 \times 10^{-3}$ for $p_T = 1$ and $p_T \in \{3, 5\}$, respectively.

As with every practical method, the L-curve has its advantages and disadvantages. There are two main disadvantages or limitations of the L-curve criterion. The first disadvantage is concerned with the reconstruction of very smooth exact solutions, see Tikhonov et al. [44]. For such solutions, Hanke [45] showed that the L-curve criterion will fail, and the smoother the solution, the worse the regularization parameter λ computed by the L-curve criterion. However, it is not clear how often very smooth solutions arise in applications. The second limitation of the L-curve criterion is related to its asymptotic behaviour as the problem size M increases. As pointed out by Vogel [46], the regularization parameter λ computed by the L-curve criterion may not behave consistently with the optimal parameter λ_{opt} as M increases. However, this ideal situation in which the same problem is discretised for increasing M may not arise so often in practice. Often the problem size M is fixed by the particular measurement setup given by N, and if a larger M is required then a new experiment must be undertaken since the inequality $M \leqslant 2N$ must be satisfied. Apart from these two limitations, the advantages of the L-curve criterion are its robustness and ability to treat perturbations consisting of correlated noise, see for more details Hansen [35].

In order to analyse the accuracy of the numerical results obtained, we introduce the errors e_T and e_Φ given by

$$e_T(\lambda) = \frac{1}{L}\left\{\sum_{l=1}^{L}\left(T^{(\text{an})}(\boldsymbol{x}^l) - T^{(\lambda)}(\boldsymbol{x}^l)\right)^2\right\}^{1/2},$$

$$e_\Phi(\lambda) = \frac{1}{L}\left\{\sum_{l=1}^{L}\left(\Phi^{(\text{an})}(\boldsymbol{x}^l) - \Phi^{(\lambda)}(\boldsymbol{x}^l)\right)^2\right\}^{1/2}, \tag{18}$$

where $\boldsymbol{x}^l$, $l = 1, \ldots, L$, are $L = 80 \times$ meas(Γ_2)/meas(Γ) uniformly distributed points on the underspecified boundary Γ_2, $T^{(\text{an})}$ and $\Phi^{(\text{an})}$ are the analytical temperature and flux on Γ_2, respectively, and $T^{(\lambda)}$ and $\Phi^{(\lambda)}$ are the numerical temperature and flux on Γ_2, respectively, obtained for the value λ of the regularization parameter.

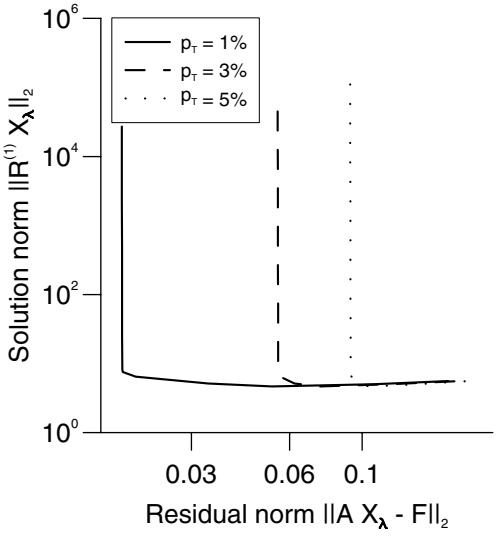

Fig. 2. The L-curves obtained for various levels of noise added into the temperature data $T|_{\Gamma_1}$, namely $p_T = 1\%$ (—), $p_T = 3\%$ (– –) and $p_T = 5\%$ (· · ·), with $M = 10$ source points, $N = 40$ boundary collocation points and $R = 5.0$ for the Example 2.

Alternatively, one can analyse the relative errors E_T and E_Φ defined by

$$E_T(\lambda) = \frac{1}{L}\left\{\sum_{l=1}^{L}\left[\left(T^{(\mathrm{an})}(\boldsymbol{x}^l) - T^{(\lambda)}(\boldsymbol{x}^l)\right) \Big/ \max_{\Gamma_2}\left|T^{(\mathrm{an})}\right|\right]^2\right\}^{1/2},$$

$$E_\Phi(\lambda) = \frac{1}{L}\left\{\sum_{l=1}^{L}\left[\left(\Phi^{(\mathrm{an})}(\boldsymbol{x}^l) - \Phi^{(\lambda)}(\boldsymbol{x}^l)\right) \Big/ \max_{\Gamma_2}\left|\Phi^{(\mathrm{an})}\right|\right]^2\right\}^{1/2}. \tag{19}$$

From expressions (18) and (19) it can be seen that the absolute, e_T and e_Φ, and the relative, E_T and E_Φ, errors differ only by a constant, i.e. $e_T = E_T \times \max_{\Gamma_2}|T^{(\mathrm{an})}|$ and $e_\Phi = E_\Phi \times \max_{\Gamma_2}|\Phi^{(\mathrm{an})}|$, and these errors have the same behaviour as functions of the regularization parameter. In addition, the relative errors given by Eq. (18) are commonly used and presented in the MFS literature, see [3–17], and therefore we restrict ourselves to analysing these errors.

Fig. 3(a) and (b) illustrate the accuracy errors e_T and e_Φ, respectively, given by relation (18), as functions of the regularization parameter λ, obtained with various levels of noise added into the input temperature data $T|_{\Gamma_1}$ for the Cauchy problem given by Example 2. From these figures it can be seen that both errors e_T and e_Φ decrease as the level of noise p_T added into the input temperature data decreases for all the regularization parameters λ and $e_T < e_\Phi$ for all the regularization parameters λ and a fixed amount p_T of noise added into the input temperature data, i.e. the numerical results obtained for the temperature are more accurate than those retrieved for the flux on the underspecified boundary Γ_2. Furthermore, by comparing Figs. 2 and 3, it can be seen, for various levels of noise, that the "corner" of the L-curve occurs at about the same value of the regularization parameter λ where the minimum in the accuracy errors e_T and e_Φ is attained. Hence the choice of the optimal regularization parameter λ_{opt} according to the L-curve criterion is fully justified. Similar results have been obtained for the Cauchy problems given by Examples 1 and 3 and therefore they are not presented here.

Figs. 4–6 illustrate the analytical and the numerical results for the temperature T and the flux Φ, obtained

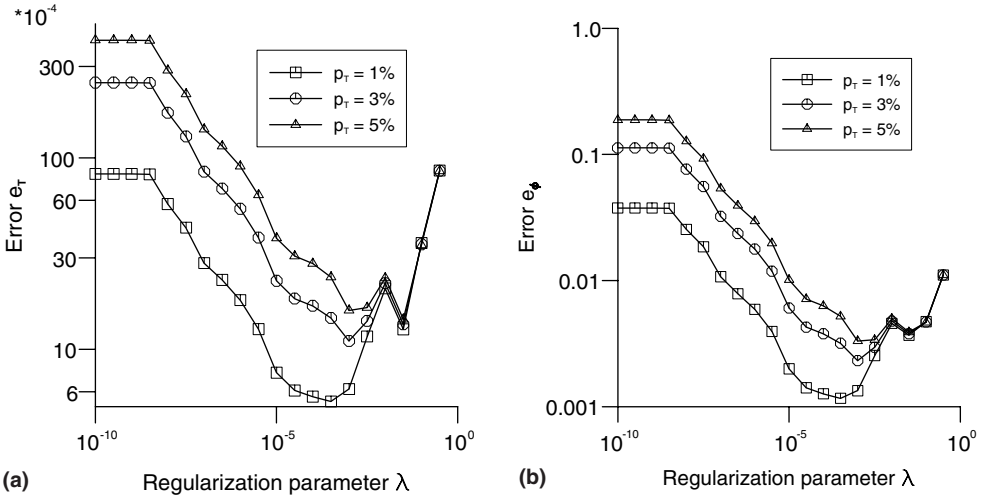

Fig. 3. The accuracy errors (a) e_T, and (b) e_Φ, as functions of the regularization parameter λ, obtained for various levels of noise added into the temperature $T|_{\Gamma_1}$, namely $p_T = 1\%$ (□), $p_T = 3\%$ (○) and $p_T = 5\%$ (△), with $M = 10$ source points, $N = 40$ boundary collocation points and $R = 5.0$ for the Example 2.

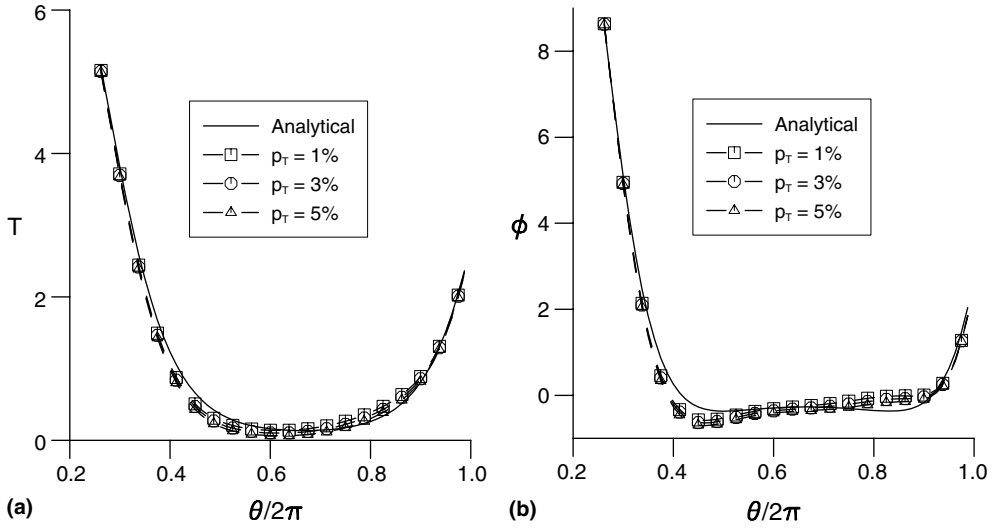

Fig. 4. (a) The analytical $T^{(an)}$ (—) and the numerical $T^{(\lambda)}$ temperatures, and (b) the analytical $\Phi^{(an)}$ (—) and the numerical $\Phi^{(\lambda)}$ fluxes, retrieved on the underspecified boundary Γ_2 with $M = 10$ source points, $N = 20$ boundary collocation points, $R = 5.0$, $\lambda = \lambda_{opt}$ and various levels of noise added into the temperature $T|_{\Gamma_1}$, namely $p_T = 1\%$ (–□–), $p_T = 3\%$ (–○–) and $p_T = 5\%$ (–△–), for the Example 1.

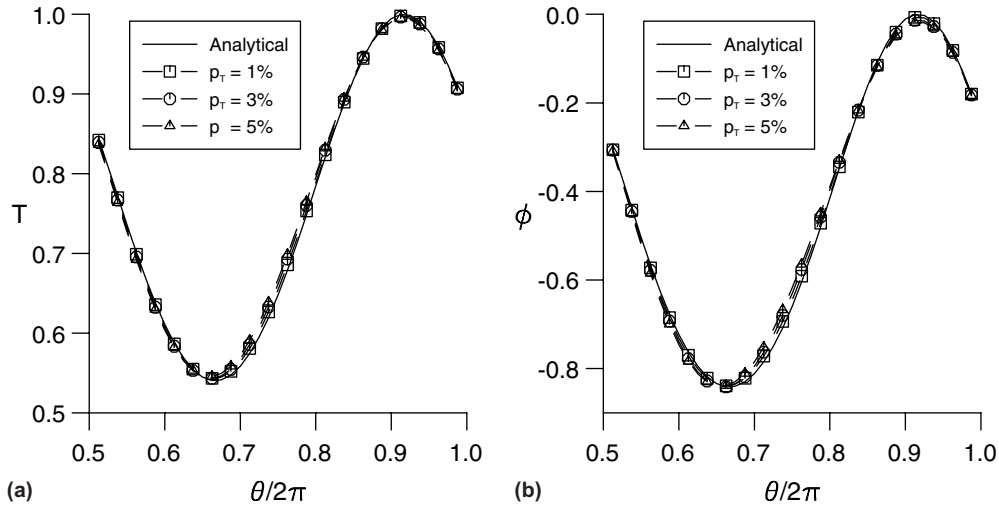

Fig. 5. (a) The analytical $T^{(an)}$ (—) and the numerical $T^{(\lambda)}$ temperatures, and (b) the analytical $\Phi^{(an)}$ (—) and the numerical $\Phi^{(\lambda)}$ fluxes, retrieved on the underspecified boundary Γ_2 with $M = 20$ source points, $N = 40$ boundary collocation points, $R = 5.0$, $\lambda = \lambda_{opt}$ and various levels of noise added into the temperature $T|_{\Gamma_1}$, namely $p_T = 1\%$ (–□–), $p_T = 3\%$ (–○–) and $p_T = 5\%$ (–△–), for the Example 2.

on the underspecified boundary Γ_2 using the optimal regularization parameter $\lambda = \lambda_{opt}$ chosen according to the L-curve criterion and various levels of noise added into the input temperature data $T|_{\Gamma_1}$, namely $p_T \in \{1, 3, 5\}$, for the Cauchy problems given by Examples 1–3, respectively. In order to get more insight into the approximation provided by the MFS in the case of the Cauchy problems under investigation, we also analyse the local relative percentage errors Err_T and Err_Φ defined as

$$\mathrm{Err}_T = \frac{|T^{(an)}(\boldsymbol{x}^l) - T^{(\lambda)}(\boldsymbol{x}^l)|}{\max_{\Gamma_2} |T^{(an)}|} \times 100,$$

$$\mathrm{Err}_\Phi = \frac{|\Phi^{(an)}(\boldsymbol{x}^l) - \Phi^{(\lambda)}(\boldsymbol{x}^l)|}{\max_{\Gamma_2} |\Phi^{(an)}|} \times 100. \tag{20}$$

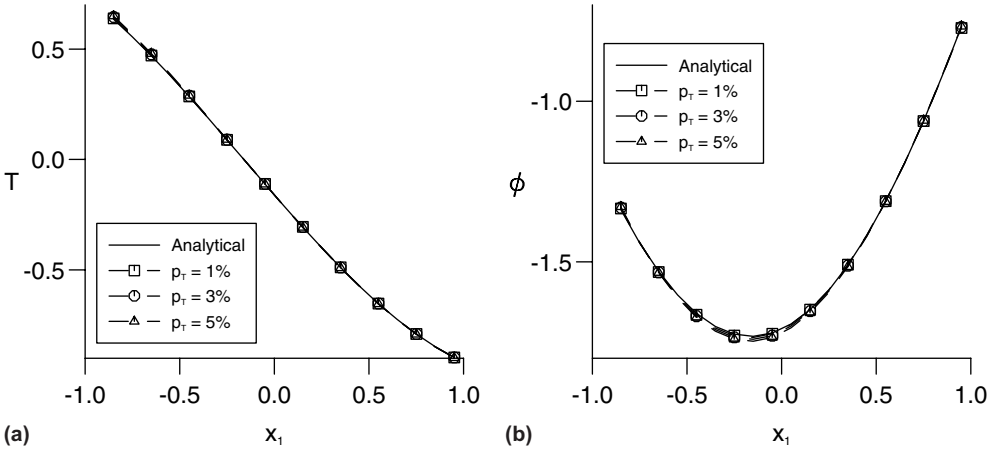

Fig. 6. (a) The analytical $T^{(an)}$ (—) and the numerical $T^{(\lambda)}$ temperatures, and (b) the analytical $\Phi^{(an)}$ (—) and the numerical $\Phi^{(\lambda)}$ fluxes, retrieved on the underspecified boundary Γ_2 with $M = 20$ source points, $N = 60$ boundary collocation points, $R = 5.0$, $\lambda = \lambda_{opt}$ and various levels of noise added into the temperature $T|_{\Gamma_1}$, namely $p_T = 1\%$ (–□–), $p_T = 3\%$ (–○–) and $p_T = 5\%$ (–△–), for the Example 3.

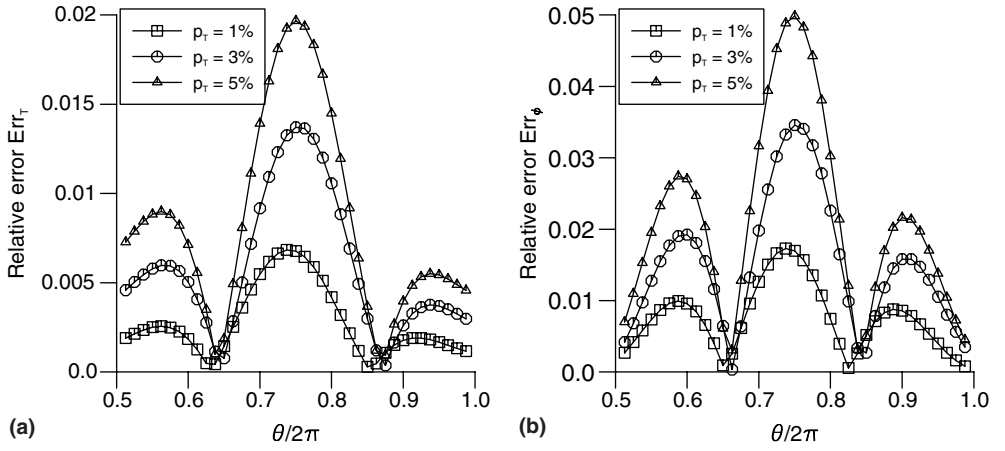

Fig. 7. The relative errors (a) Err_T, and (b) Err_Φ, retrieved on the underspecified boundary Γ_2 with $M = 20$ source points, $N = 40$ boundary collocation points, $R = 5.0$, $\lambda = \lambda_{opt}$ and various levels of noise added into the temperature $T|_{\Gamma_1}$, namely $p_T = 1\%$ (–□–), $p_T = 3\%$ (–○–) and $p_T = 5\%$ (–△–), for the Example 2.

Fig. 7(a) and (b) present the local relative percentage errors Err_T and Err_Φ given by relation (20), obtained on the underspecified boundary Γ_2 using the optimal regularization parameter $\lambda = \lambda_{opt}$ chosen according to the L-curve criterion and various levels of noise added into the input temperature data $T|_{\Gamma_1}$, namely $p_T \in \{1, 3, 5\}$, for the Cauchy problem given by Example 2. It can be seen from this figures that the MFS approximation provides very accurate numerical results for both the temperature and the flux on the underspecified boundary Γ_2, in the sense that the errors Err_T and Err_Φ are $O(10^{-2})$. Furthermore, both errors Err_T and Err_Φ decrease as the level of noise p_T added into the input temperature data decreases and $Err_T < Err_\Phi$ for a fixed amount p_T of additive noise, i.e. the numerical results retrieved for the temperature are more accurate than those obtained for the flux on the boundary Γ_2. Similar results have been obtained for the other examples and therefore they are not presented herein. From Figs. 4–7 we can conclude that the numerical solutions retrieved for all examples investigated in this study are accurate and stable with respect to the amount of noise p_T added into the input temperature data $T|_{\Gamma_1}$.

4.2. Convergence of the method

In order to investigate the influence of the number M of source points on the accuracy and stability of the

numerical solutions for the temperature and the flux on the underspecified boundary Γ_2, we set $R = 5.0$ for the Example 1 and $p_T = 5$. In Fig. 8(a) and (b) we present the accuracy errors e_T and e_Φ for the Example 1, respectively, as functions of the number M of source points, obtained using $\lambda = \lambda_{\text{opt}}$ given by the L-curve criterion. It can be seen from these figures that both accuracy errors tend to zero as the number M of source points increases and, in addition, these errors do not decrease substantially for $M \geq 10$. These results indicate the fact that the MFS in conjunction with the first-order Tikhonov regularization method provides accurate and convergent numerical solutions with respect to increasing the number of source points, with the mention that a small number of source points is required in order for a good accuracy of the numerical temperature and flux on the boundary Γ_2 to be achieved.

Next, we analyse the convergence of the numerical method proposed with respect to the position of the source points. To do so, we set $M = 20$ and $p_T = 5$ for the Cauchy problem given by Example 3, while at the same time varying the radius R. Fig. 9(a) and (b) illustrate the accuracy errors e_T and e_Φ for the Example 3, respectively, as functions of R, obtained using $\lambda = \lambda_{\text{opt}}$ given by the L-curve criterion. From these figures it can be seen that the larger is the distance from the source

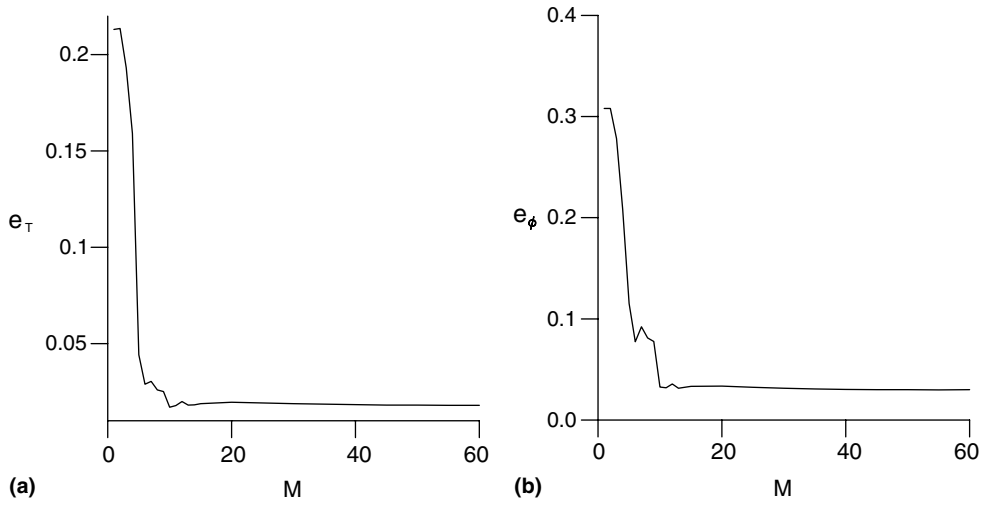

Fig. 8. The accuracy errors (a) e_T, and (b) e_Φ, obtained with $N = 20$ boundary collocation points, $R = 5.0$, $\lambda = \lambda_{\text{opt}}$ and $p_T = 5\%$ for the Example 1, as functions of the number M of source points.

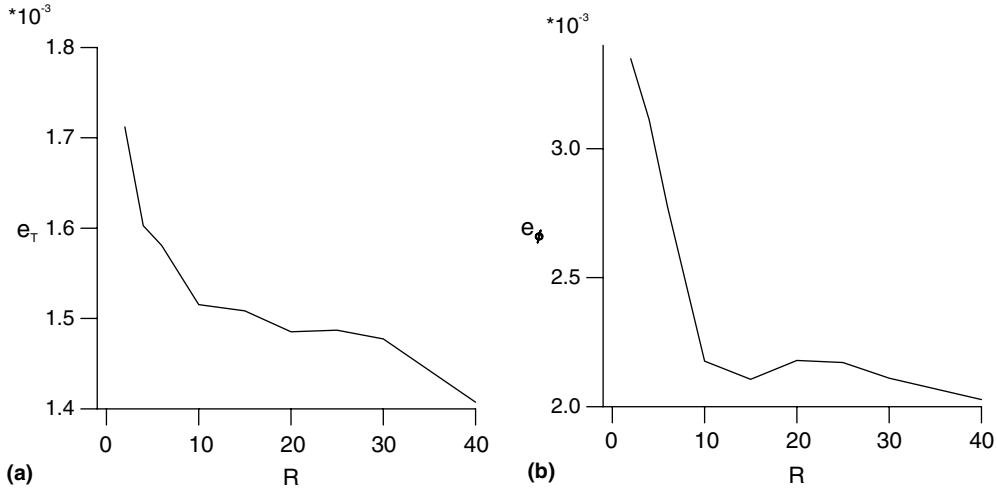

Fig. 9. The accuracy errors (a) e_T, and (b) e_Φ, obtained with $M = 60$ source points, $N = 20$ boundary collocation points, $\lambda = \lambda_{\text{opt}}$ and $p_T = 5\%$ for the Example 3, as functions of the distance R between the source points and the boundary Γ of the solution domain Ω.

points to the boundary Γ of the solution domain Ω, i.e. the larger is R, the better the accuracy in the numerical temperatures and fluxes. It should be noted that the value $R = 10$ was found to be sufficiently large such that any further increase in this distance between the source points and the boundary Γ did not significantly improve the accuracy of the numerical results for the Example 3. Although not presented here, it is reported that similar results have been obtained for all examples analysed in this study and hence we can conclude that the numerical method proposed is convergent with respect to increasing the number of source points and the distance between the source points and the boundary of the solution domain.

5. Conclusions

In this paper, the Cauchy problem associated with two-dimensional Helmholtz-type equations has been investigated by employing the MFS. The resulting ill-conditioned system of linear algebraic equations has been regularized by using the first-order Tikhonov regularization method, while the choice of the optimal regularization parameter was based on the L-curve criterion. Three benchmark examples involving both the Helmholtz and the modified Helmholtz equations in smooth and piecewise smooth geometries have been analysed. The numerical results obtained show that the proposed method is convergent with respect to increasing the number of source points and the distance from the source points to the boundary of the solution domain and stable with respect to decreasing the amount of noise added into the input data. Moreover, the method is efficient, easy to adapt to three-dimensional Cauchy problems associated with Helmholtz-type equations, as well as to complex and irregular domains, but these investigations are deferred to future work.

Acknowledgment

Liviu Marin would like to acknowledge the financial support received from the EPSRC.

References

[1] Kupradze VD, Aleksidze MA. The method of functional equations for the approximate solution of certain boundary value problems. USSR Comput Math Math Phys 1964;4:82–126.

[2] Mathon R, Johnston RL. The approximate solution of elliptic boundary value problems by fundamental solutions. SIAM J Numer Anal 1977;14:638–50.

[3] Fairweather G, Karageorghis A. The method of fundamental solutions for elliptic boundary value problems. Adv Comput Math 1998;9:69–95.

[4] Balakrishnan K, Ramachandran PA. A particular solution Trefftz method for non-linear Poisson problems in heat and mass transfer. J Comput Phys 1999;150:239–67.

[5] Golberg MA, Chen CS. Discrete projection methods for integral equations. Southampton: Computational Mechanics Publications; 1996.

[6] Golberg MA, Chen CS. The method of fundamental solutions for potential, Helmholtz and diffusion problems. In: Golberg MA, editor. Boundary integral methods: numerical and mathematical aspects. Boston: WIT Press and Computational Mechanics Publications; 1999. p. 105–76.

[7] Karageorghis A, Fairweather G. The method of fundamental solutions for the numerical solution of the biharmonic equation. J Comput Phys 1987;69:434–59.

[8] Poullikkas A, Karageorghis A, Georgiou G. Methods of fundamental solutions for harmonic and biharmonic boundary value problems. Comput Mech 1998;21:416–23.

[9] Poullikkas A, Karageorghis A, Georgiou G. The method of fundamental solutions for inhomogeneous elliptic problems. Comput Mech 1998;22:100–7.

[10] Poullikkas A, Karageorghis A, Georgiou G. The numerical solution of three-dimensional Signorini problems with the method of fundamental solutions. Eng Anal Boundary Elem 2001;25:221–7.

[11] Karageorghis A, Fairweather G. The method of fundamental solutions for axisymmetric elasticity problems. Comput Mech 2000;25:524–32.

[12] Berger JA, Karageorghis A. The method of fundamental solutions for heat conduction in layered materials. Int J Numer Meth Eng 1999;45:1681–94.

[13] Berger JA, Karageorghis A. The method of fundamental solutions for layered elastic materials. Eng Anal Boundary Elem 2001;25:877–86.

[14] Karageorghis A. The method of fundamental solutions for the calculation of the eigenvalues of the Helmholtz equation. Appl Math Lett 2001;14:837–42.

[15] Poullikkas A, Karageorghis A, Georgiou G. The numerical solution for three-dimensional elastostatics problems. Comput Struct 2002;80:365–70.

[16] Ramachandran PA. Method of fundamental solutions: Singular value decomposition analysis. Commun J Numer Meth Eng 2002;18:789–801.

[17] Balakrishnan K, Sureshkumar R, Ramachandran PA. An operator splitting-radial basis function method for the solution of transient nonlinear Poisson problems. Comput Math Appl 2001;43:289–304.

[18] Beskos DE. Boundary element method in dynamic analysis: Part II (1986–1996). ASME Appl Mech Rev 1997;50:149–97.

[19] Chen JT, Wong FC. Dual formulation of multiple reciprocity method for the acoustic mode of a cavity with a thin partition. J Sound Vib 1998;217:75–95.

[20] Harari I, Barbone PE, Slavutin M, Shalom R. Boundary infinite elements for the Helmholtz equation in exterior domains. Int J Numer Meth Eng 1998;41:1105–31.

[21] Hall WS, Mao XQ. A boundary element investigation of irregular frequencies in electromagnetic scattering. Eng Anal Boundary Elem 1995;16:245–52.

[22] Kern DQ, Kraus AD. Extended surface heat transfer. New York: McGraw-Hill; 1972.

[23] Niwa Y, Kobayashi S, Kitahara M. Determination of eigenvalue by boundary element method. In: Banerjee PK, Shaw R, editors. Development in Boundary Element Methods. New York: Applied Science Publisher; 1982. Chapter 7.
[24] Nowak AJ, Brebbia CA. Solving Helmholtz equation by boundary elements using multiple reciprocity method. In: Calomagno GM, Brebbia CA, editors. Computer experiment in fluid flow. Berlin: CMP/Springer Verlag; 1989. p. 265–70.
[25] Agnantiaris JP, Polyzer D, Beskos D. Three-dimensional structural vibration analysis by the dual reciprocity BEM. Comput Mech 1998;21:372–81.
[26] Hadamard J. Lectures on Cauchy problem in linear partial differential equations. London: Oxford University Press; 1923.
[27] Bai MR. Application of BEM-based acoustic holography to radiation analysis of sound sources with arbitrarily shaped geometries. J Acoust Soc Am 1992;92:533–49.
[28] Kim BK, Ih JG. On the reconstruction of the vibro-acoustic field over the surface enclosing an interior space using the boundary element method. J Acoust Soc Am 1996;100:3003–16.
[29] Wang Z, Wu SR. Helmholtz equation-least-squares method for reconstructing the acoustic pressure field. J Acoust Soc Am 1997;102:2020–32.
[30] Wu SR, Yu J. Application of BEM-based acoustic holography to radiation analysis of sound sources with arbitrarily shaped geometries. J Acoust Soc Am 1998;104:2054–60.
[31] DeLillo T, Isakov V, Valdivia N, Wang L. The detection of the source of acoustical noise in two dimensions. SIAM J Appl Math 2001;61:2104–21.
[32] Marin L, Elliott L, Heggs PJ, Ingham DB, Lesnic L. An alternating iterative algorithm for the Cauchy problem associated to the Helmholtz equation. Comput Meth Appl Mech Eng 2003;192:709–22.
[33] Marin L, Elliott L, Heggs PJ, Ingham DB, Lesnic L. Conjugate gradient-boundary element solution to the Cauchy problem for Helmholtz-type equations. Comput Mech 2003;31:367–77.
[34] Tikhonov AN, Arsenin VY. Methods for solving ill-posed problems. Moscow: Nauka; 1986.
[35] Hansen PC. The L-curve and its use in the numerical treatment of inverse problems. In: Johnston P, editor. Computational inverse problems in electrocardiology. Southampton: WIT Press; 2001. p. 119–42.
[36] Chen G, Zhou J. Boundary element methods. London: Academic Press; 1992.
[37] Katsurada M, Okamoto H. A mathematical study of the charge simulation method. J Fac Sci, Univ Tokyo, Sect 1A, Math 1988;35:507–18.
[38] Katsurada M. A mathematical study of the charge simulation method II. J Fac Sci, Univ Tokyo, Sect 1A, Math 1989;36:135–62.
[39] Katsurada M. Asymptotic error analysis of the charge simulation method in Jordan region with an analytic boundary. J Fac Sci, Univ Tokyo, Sect 1A, Math 1990;37:635–57.
[40] Katsurada M. Charge simulation method using exterior mapping functions. Jpn J Ind Appl Math 1994;11:47–61.
[41] Kondepalli PS, Shippy DJ, Fairweather G. Analysis of acoustic scattering in fluids and solids by the method of fundamental solutions. J Acoust Soc Am 1992;91:1844–54.
[42] MacDonell M. A boundary method applied to the modified Helmholtz equation in three dimensions and its application to a waste disposal problem in the deep ocean. MSc Thesis, Department of Computer Science, University of Toronto, 1985.
[43] Hansen PC. Rank-deficient and discrete ill-posed problems: numerical aspects of linear inversion. Philadelphia: SIAM; 1998.
[44] Tikhonov AN, Leonov AS, Yagola AG. Nonlinear ill-posed problems. London: Chapman & Hall; 1998.
[45] Hanke M. Limitations of the L-curve method in ill-posed problems. BIT 1996;36:287–301.
[46] Vogel CR. Non-convergence of the L-curve regularization parameter selection method. Inverse Prob 1996;12:535–47.